PHYSICAL REVIEW C VOLUME 25, NUMBER 5 MAY 1982

Inclusion of deuteron and alpha-particle collisions in intranuclear cascade calculations

G. J. Mathews
University of California, Lawrence Livermore National Laboratory, Livermore, California 94550

B. G. Glagola
Chemistry Division, Argonne National Laboratory, Argonne, Illinois 60514

R. A. Moyle
Scientific Applications, Inc., McLean, Virginia 22101

V. E. Viola, Jr.
Chemistry Department, Indiana University, Bloomington, Indiana 47405
(Received 25 September 1981)

An intranuclear cascade model generalized to allow deuteron and alpha-particle collisions during the cascade is discussed. A comparison of calculations is presented for nucleon-induced cascades with and without clusters present in the target nucleus and the effects of clustering are inferred. Alpha-particle-induced collisions are studied in detail and compared with experimental data. It is found that many features of alpha-particle-induced reactions can be well understood with this model. Possible shortcomings and directions of future improvements in the code are highlighted.

[NUCLEAR REACTIONS Intranuclear cascade models; effects of including d and α as incident projectiles or preformed clusters.]

I. INTRODUCTION

Interactions between complex nuclei and light-ion projectiles are of interest from many points of view. The underlying motivation for studying such reactions is to understand the sequence of events whereby the energy of the projectile is distributed among the internal degrees of freedom of the target-projectile system. The nature of the energy, mass, charge, and angular distributions of the reaction products, including both light-particle spectra and spallation residues, reflect these processes. Despite extensive theoretical and experimental effort, only limited success has been achieved thus far in describing these features of light-ion-induced reactions at intermediate energies. In view of the present high interest in the study of reactions induced by complex nuclei with similar energies, i.e., 20–200 MeV/nucleon, the need for an improved understanding of the simpler light-ion systems in the same E/A region seems apparent. In addition, these reactions are also of practical significance in the search for rare nuclei far from beta stability, astrophysical problems relating to cosmic ray transport, and studies of the biological effects of penetrating radiation.

Attempts to describe light-ion interactions at intermediate and high energies have generally involved a two-step reaction mechanism.[1,2] The first stage in these models involves a sequence of nucleon-nucleon collisions which transfer energy to the target nucleus on a fast time scale. Subsequently, the excited residual nucleus undergoes energy equilibration and decays via particle evaporation and gamma-ray emission.

Over the years a number of models based on Monte Carlo techniques have been developed in order to describe the initial intranuclear cascade phase of such reactions.[3–10] These models involve approximate forms of the nuclear potential and nucleon density distribution and keep track of sequential collisions at each stage in the cascade. The scattering process is described by the inclusions of

differential cross sections for free nucleon-nucleon scattering as a function of energy. Only collisions consistent with the Pauli exclusion principle are allowed. These models have met with a degree of success that might be expected in view of the many approximations to the physics of intermediate-to-high-energy collisions. In general, their ability to predict total cross sections for a given product can be correct to within about a factor of 2, but discrepancies may arise when comparisons are made with angular distributions and energy spectra of the product nuclei.[7,8] Clearly refinements in the description of the intranuclear cascade are needed.

A highly desirable improvement in these intranuclear cascade models would be the inclusion of more complex particles (e.g., ^{2}H and ^{4}He) as incident projectiles in the cascade. This generalization should facilitate a better kinematic understanding of experimental data involving complex projectiles at intermediate energies. Although the main purpose of this paper is to study the effects of complex projectiles on the cascade, at the same time we can also study the possible influence on the cascade owing to preformed bound clusters in the target nucleus. That such clusters may exist in nuclei has been suggested in the context of Hartree-Fock theory where it is observed that nucleons may group together into two alpha-particle clusters in some light nuclei.[11] Also, it has been proposed[12] that the low-density surface regions of heavy nuclei may be conducive to alpha-particle cluster formation. In the nuclear interior, clusters may be manifest as the fraction of phase space which corresponds to nucleons moving with low relative Fermi momenta, even if composites do not exist as density fluctuations. The intention of the schematic study presented here will be to highlight possible experimental signatures of clustering in nuclei, if it exists, which might be observable in the background from nucleon-nucleon collisions or from composite formation by coalescence (which is not considered here).

The new version of the cascade code described here includes all possible collision pairs for p, n, d, and α. The approach of this paper is first to compare the modified code with previous calculations[8] of nucleon-induced collisions in order to demonstrate the salient features introduced by nucleon clustering, and then to make detailed comparisons with experimental data for alpha-particle-induced collisions. An overview of the model is presented in Sec. II. The comparison with other cascade codes and experimental data is presented in Secs. III and IV.

II. THE MODEL

As a starting point for the inclusion of complex particles in the intranuclear cascade model, the code of Chen *et al.*[7] has been adopted. The physics contained in this code includes a diffuse nuclear surface and the possibility of reflection or refraction in regions of changing nuclear density. Since a detailed account of the Chen *et al.* code exists in the literature,[7,8] the discussion here is confined to those features of the calculation which have been generalized to accommodate collisions involving deuterons and alpha particles.

A. Collisions during the cascade

In the cascade codes which have been constructed to date, it is assumed that the sequence of collisions can be described by classical trajectories resulting from free nucleon-nucleon interactions. Two important underlying assumptions are (1) the de Broglie wavelength of the incident particle is small compared to other relevant distances (e.g., the mean free path), so that a classical trajectory is appropriate, and (2) correlations among nucleons enter only through the Pauli principle and average binding energies, permitting a free scattering description of the system. The introduction of clustering should further correct for correlations in the sense that a collision with a single nucleon may also affect the motion of other nucleons in the nucleus. Even though the mean free path of clusters is considerably reduced, the de Broglie wavelength is also reduced. Therefore we apply the classical trajectory and free scattering description to the clusters. The collision pairs which have been added to the cascade code include: p-d, n-d, p-α, d-d, d-α, and α-α.

1. Scattering cross sections

Total cross sections and center-of-mass differential cross sections for scattering of the collision pairs listed above were added to the code based on data in Refs. 13–29 and the references therein. Smooth extrapolations to 400 MeV were made for cases where data were not available. Since the Chen *et al.* code is valid only up to the pion threshold, scattering cross sections beyond 400 MeV were not included. In some cases the total cross sections were generated by performing an optical model fit to elastic scattering data. It was assumed that the

p-d and n-d cross sections were identical; a similar assumption was made for p-α and n-α collisions.

2. Breakup

One complication expected to arise during the collision process is that the cluster may break up into its constituent nucleons or other clusters during the cascade. Hence, after a cluster collision, it is uncertain as to whether to follow the trajectory of the original cluster or individual nucleons. In this case we have introduced the simplest possible picture, short of neglecting breakup altogether. Since the simple clusters considered in this model have only a single bound state, the probability P of cluster breakup can be approximated by

$$P=\sigma_R(E)/\sigma_T(E)\ , \tag{1}$$

where σ_R is the reaction cross section and σ_T is the total geometric scattering cross section

$$\sigma_T=\pi R^2;\ \ R=1.2(A_1{}^{1/3}+A_2{}^{1/3})\ \text{fm}\ .$$

Some of the values of the quantity P derived from the literature are shown in Fig. 1 as a function of center-of-mass energy above the threshold for the reaction. The point to note here is that P appears to be essentially independent of the cluster partners in the collision.

In tracking the cascade sequence involving clusters, the probability for cluster breakup is determined according to the step function in Fig. 1. Random number selection is the criterion for deciding whether a breakup has occurred. The energy balance is accounted for by allowing the energy of the collision to go into thermal excitation of the residual nucleus. At this point the cluster is considered to be completely absorbed and is no longer followed in the cascade. A more rigorous approach would be to follow each exit particle through the cascade; however, this is a time-consuming task beyond the computer capability of the present calculation.

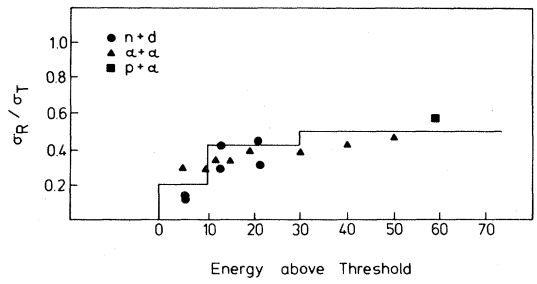

FIG. 1. Step function used to calculate cluster breakup probability ($\sigma_R/\sigma_{\text{tot}}$) as a function of the cluster energy above breakup threshold.

3. Choice of cluster

The choice of collision partner type (n, p, d, or α) for reactions in which clusters are allowed to exist in the target is determined by random number selection and the relative spectroscopic factors for the target. The kinematics of the collision are determined according to the procedure outlined by Chen *et al.*[7] The cascade stops when the energy of the nucleon or cluster is below a cutoff energy. The cutoff energy (as in Chen *et al.*[7]) is taken here as two times the average binding energy of the particle (cluster) or the sum of the binding energy plus the Coulomb barrier energy, whichever is the larger. These are tabulated in Table I for the systems calculated here. Particles (clusters) with energies below the cutoff are assumed to be absorbed by the target and are no longer followed in the cascade.

B. Cluster density distributions

In the Chen *et al.* code the nuclear density distribution is described by a series of eight concentric shells of constant density which approximate the measured nuclear charge distribution function. However, the density distribution of the clusters within the nucleus is not *a priori* clear. Clustering may be enhanced on the nuclear surface and indeed studies of cluster knockout reactions have demonstrated that the knockout reaction is surface peaked.[13] The observed surface peaking at high incident energy seems reasonably well understood from shell-model spectroscopic factors and is therefore not necessarily a manifestation of the cluster density distribution but may simply relate to the short mean-free-path of the cluster.[30] Therefore we choose a simple physical picture which is consistent with the data and the scope of the intranuclear cascade model.

In the cascade model the nucleons are treated as a degenerate gas of fermions which therefore occupy well-defined orbits. It can be postulated that there is a finite probability for the wave functions of two or more individual fermions to overlap in a zero relative momentum state [e.g., $(1s)^n$ for n nucleons]. A cluster is defined in this context. The wave function and spectroscopic factor for such a cluster

TABLE I. Average binding energies B_i, Coulomb barrier energies V_i, and cutoff energies, CE_i, for ^{27}Al and ^{181}Ta used in these calculations (in MeV).

	B_p	B_n	B_d	B_α
^{27}Al	8.3	8.1	14.1	5.1
^{181}Ta	6.5	7.0	11.2	1.8
	V_p	V_n	V_d	V_α
^{27}Al	3.4	0	3.4	6.8
^{181}Ta	12.6	0	12.6	25.2
	CE_p	CE_n	CE_d	CE_α
^{27}Al				
CLUST	10.3	16.1	28.2	11.9
ORNL	10.3	7.0		
JIRN	8.9	7.0		
BNL-CU	12.4	9.1		
^{181}Ta				
CLUST	19.3	19.1	23.8	27.0
ORNL	19.3	7.0		
JINR	13.8	7.0		
CNL-CU	19.3	7.0		

could be generated, for example, by transforming the nucleon shell-model wave functions into the center-of-mass motion of the cluster and the relative coordinates of the cluster nucleons. Because this is just a coordinate transformation, physical observables, such as the density distributions, are invariant, and the cluster density distributions are therefore expected to track the nucleon distribution. It is thus assumed in this model that the cluster density is the same as the nucleon density distribution. To date, we have not investigated the effects of different cluster density functions (e.g., surface peaked or a cluster distribution that extends to larger radii than the nucleon distribution).

The principal question that remains relates to the relative amplitudes for the cluster and single-particle wave functions. An exact calculation of these quantities is beyond the scope of this code. Consequently, the effective number of deuteron and alpha-particle clusters in a nucleus is treated as an empirical factor for comparison with calculations which do not include clusters.[8] In general, for these comparisons a relatively larger cluster number is used to demonstrate the differences between cluster and noncluster versions of the code and to help elucidate the effects resulting from the inclusion of clusters. For direct comparison to experimental data, either experimental spectroscopic factors are needed or the cluster number can be used as a free parameter to fit the data.

C. Cluster momentum and energy distribution

In the intranuclear cascade code of Chen *et al.*,[7] the momenta of the nucleons in each density region are given by the Fermi momentum corresponding to that density. The cluster momentum distribution is not easily defined. Since deuterons and alpha particles have integer spins, they should obey Bose-Einstein statistics (at least in the low-density limit). In regions of high nuclear matter density as the clusters overlap, the intrinsic fermionic structure of the clusters promotes constituent nucleons to higher momentum states. This picture is supported by the well-known result that bringing two alpha particles in close contact is equivalent to placing four nucleons in the *s-d* shell of an oscillator well whose 1*s* state is occupied by one of the alpha particles. For simplicity we assume this picture to determine the cluster momenta, with the caveat that this may not be appropriate in the low-density surface regions of

the nucleus. Hence, in the framework of this model, the Fermi momentum p_f (or Fermi energy E_f) of an n-nucleon cluster will be taken as n times the Fermi momentum (or energy) of an individual nucleon. Once the kinetic energy of the cluster is defined in this way, the potential energy of the cluster in the nucleus is given as in Chen *et al.* by

$$-V=E_f+E_B \ ,$$

where E_B is the binding energy of the most weakly bound deuteron or alpha-particle cluster for nuclei in the mass region of the target nucleus. As in the nucleon-nucleon case, a Pauli-exclusion requirement exists for clusters such that a collision is not allowed unless both partners recoil with an energy greater than their respective Fermi energies. Ultimately, the Fermi energy of the collision partners determines whether or not a collision is allowed.

D. Quantities calculated by the cluster code

The cluster code is designed to account for the cascade step in nuclear reactions induced by nucleons, deuterons, and alpha particles at energies well above the Coulomb barrier. The code predicts the total cross section as well as differential cross sections, angular distributions, and energy spectra for emitted nucleons, deuterons, alpha particles, and target spallation residues. In addition, the excitation energy of each residual is stored, which permits calculation of the deexcitation process. In the second stage of the reaction we have employed the evaporation code of Dostrovsky *et al.*[9] for medium to heavy nuclei ($A>20$) and a Fermi-breakup model[31,32] for lighter nuclei. In the present paper the results of the intranuclear cascade part of the calculation for the $p+^{27}$Al and $p+^{181}$Ta systems are compared with results of other intranuclear cascade codes, and comparisons of experimental data with calculations for the $\alpha+^{27}$Al and $\alpha+^{235}$U are presented. More complete fits to experimental data will be presented in a subsequent paper.

III. NUCLEON-INDUCED CASCADES

First we consider the effect of preformed clusters on nucleon-induced reactions. In order to evaluate the differences between the cluster code and existing cascade codes based on nucleon-nucleon collisions, the review of Barashenkov *et al.*[8] has been used as a basis for comparison. Three existing nucleon-nucleon codes were compared in this reference for the $p+^{27}$Al and $p+^{181}$Ta reactions at 150 and 300 MeV. These included the codes of Bertini,[4] Chen *et al.*,[7] and Barashenkov,[33] designated ORNL, BNL-CU, and JINR, respectively. The BNL-CU code is identical to the CLUST code when only nucleon-nucleon collisions are allowed. The similarities and differences among these three codes are examined in Ref. 8 and we present results for proton-induced reactions relevant to this reference.

The cluster code (CLUST) has been run for these cases in order to examine the effects of clusters on the angular and energy distributions of the emitted protons and heavy residual nuclei. Unless otherwise specified, we have used the STEPNO version of the BNL-CU code, which does not allow for refraction and reflection of particles at the nuclear potential boundaries. In Ref. 8 it was shown that the STEPNO version of the BNL-CU code and the ORNL code are nearly identical. The relative cluster density has been arbitrarily chosen to exaggerate the cluster spectroscopic factors in order to emphasize the differences between the codes. Variable spectroscopic factors which specify alpha-particle and deuteron clusters in the target nuclei were chosen for this purpose.

A. Reaction cross sections and particle multiplicities

In Table II we list the total reaction cross sections (defined as the fraction of incident particles which undergo at least one collision times the geometric cross section) obtained from calculations with the CLUST code with various assumptions about the spectroscopic factors for deuteron and alpha-particle clusters. The nomenclature is defined so that $1d$, 2α, and $3d\,3\alpha$ refer to one deuteron cluster, two alpha-particle clusters, and three deuteron plus three alpha-particle clusters, respectively, present in the target nucleus. Also shown in Table II are the multiplicities, $\bar{\nu}_i$, for the emission of light ions in the cascade.

From examination of Table II several features of the CLUST model become immediately obvious. First of all, the inclusion of clusters most dramatically affects the cross section and multiplicities for the ^{27}Al target. This is consistent with the fact that, for the choice of cluster spectroscopic factors employed here, the clusters occupy a proportionately larger fraction of the available nucleons. It is observed that the reaction cross section in general in-

TABLE II. Calculated reaction cross sections σ_R in millibarns and average particle multiplicities for the emission of cascade protons, $\bar{\nu}_p$; neutrons, $\bar{\nu}_n$; deutrons, $\bar{\nu}_d$, alpha particles, $\bar{\nu}_\alpha$, in proton-induced reactions on ^{27}Al and ^{181}Ta.

Projectile	Target	Clusters	σ_R (mb)	$\bar{\nu}_p$	$\bar{\nu}_n$	$\bar{\nu}_d$	$\bar{\nu}_\alpha$
150-MeV p	^{27}Al	0	450	0.84	0.68	0	0
		1α	512	0.81	0.51	0	0.022
		$3d$	449	0.74	0.47	0.019	0
		3α	717	0.72	0.18	0	0.038
		$3d\,3\alpha$	678	0.47	0.12	0.007	0.021
	no breakup	$3d\,3\alpha$	693	0.65	0.17	0.058	0.056
300-MeV p	^{27}Al	0	346	1.21	0.92	0	0
		$3d$	375	0.98	0.68	0.060	0
		3α	665	0.83	0.19	0	0.027
		$3d\,3\alpha$	707	0.75	0.12	0.019	0.031
	no breakup	$3d\,3\alpha$	612	0.83	0.109	0.11	0.077
150-MeV p	^{181}Ta	$2d$	1402	0.39	0.77	0.005	0
		5α	1517	0.32	0.57	0	0.001
	no breakup	5α	1657	0.39	0.64	0	0.001
300-MeV p	^{181}Ta	5α	1512	0.67	0.75	0	0.017
	no breakup	5α	1554	0.71	0.89	0	0.009
150-MeV p	^{27}Al	exp[a]	400				
156-MeV p	^{27}Al	exp[b]	356				
185-MeV p	^{27}Al	exp[c]	408				
		ORNL[d]	417				
305-MeV p	^{27}Al	exp[c]	334				
		ORNL[d]	394				

[a]Reference 31.
[b]Reference 32.
[c]Reference 33.
[d]Reference 4.

creases as the amount of cluster structure increases. Since collisions involving clusters include not only elastic scattering from the cluster, but also inelastic cluster-breakup reactions, at each step in the cascade a larger effective total cross section (compared to that for nucleon-nucleon collisions) is used to decide whether or not an interaction occurs. Thus, increasing the number of clusters increases the probability that the incident particle will undergo an interaction with the target nucleus and thereby increases the reaction cross section.

In examining the particle multiplicity results, it is observed that increasing the number of clusters decreases the average number of emitted protons and neutrons significantly. This behavior presumably results from the decreased number of free nucleons, and decreased nuclear transparency. In addition, in collisions of the incident protons with clusters, subsequent cluster collisions are less effective in ejecting additional nucleons from the nucleus during the cascade. As a consequence, one expects the inclusion of clusters to increase the internal excitation energy of the residual nuclei, as shown below.

Some experimental data[34–36] for the reaction cross sections are shown at the bottom of Table II for 150-, 156-, 185-, and 305-MeV protons incident on ^{27}Al. Also shown at the bottom of Table II are the reaction cross sections predicted by the ORNL code (which are similar to the predictions of the BNL-CU code). In comparing with these data, it can be seen that both codes overestimate the cross section. The calculations for no clusters or only three deuteron clusters appear to be in fairly good agreement. At both energies the agreement with the data is poorer as the amount of clustering is increased.

As far as the emission of deuterons and alpha particles during the cascade is concerned, we see from the multplicities in Table II that very few clusters emerge from a nucleon-induced cascade, so that the emission of complex particles will be completely dominated by coalescence in the exit channel or the evaporation step.[37] The reasons for this can be traced not only to breakup of the clusters, but also to the lower recoil energies and much shorter

mean free path for the complex particles so that only surface interactions could lead to the emission of cascade deuterons or alpha particles.

Enhanced complex particle emission in the cascade step could be realized by incorporating a coalescence relationship for cascade nucleons.[37]

B. Charged particle spectra

In Figs. 2–5 the spectra of cascade protons emitted at 30°±5° and 80°±5° are shown for both the BNL-CU (no clusters) calculation of Ref. 8 and the present CLUST code. The systems chosen for study are 150- and 300-MeV protons plus ^{27}Al and ^{181}Ta. These are the systems studied in Ref. 8 so that the reader can readily compare the results of the CLUST code with the other codes studied in that work.

To understand the differences between the calculations with and without clusters present in the nucleus, it is first necessary to understand the output of the simple nucleon-nucleon cascade. The 30° and 80° spectra for both the Al and the Ta reactions exhibit a peak near the kinematic energy for free nucleon scattering for these respective angles. This peak is broadened and skewed both by the intrinsic Fermi motion of the nucleons and by multiple scattering during the cascade. Clusters introduce both kinematic effects from the scattering of parti-

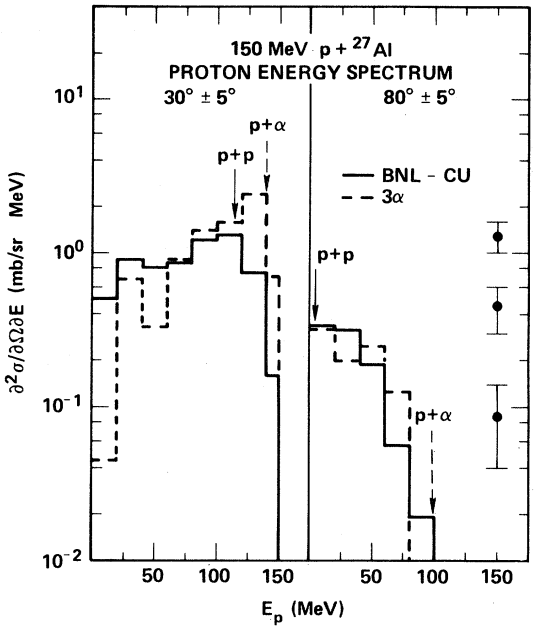

FIG. 2. Calculated energy spectra for protons emitted at 30° and 80° for the 150-MeV $p+^{27}$Al reaction. The BNL-CU results of Ref. 8 (solid line) are compared with the CLUST code (dashed line) assuming three alpha particles in the target. Representative statistical errors in the calculations are also shown. The arrows indicate the kinematic energies for free p+nucleon and $p+\alpha$ scattering.

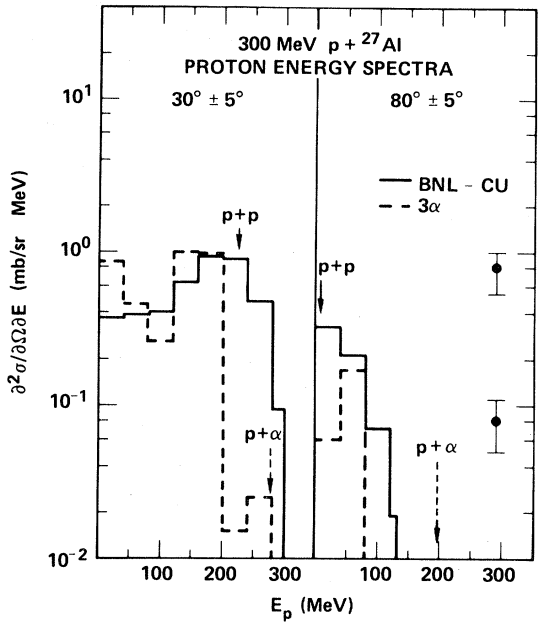

FIG. 3. Calculated energy spectra for protons emitted at 30° and 80° in the 300-MeV $p+^{27}$Al system. See Fig. 2 for details.

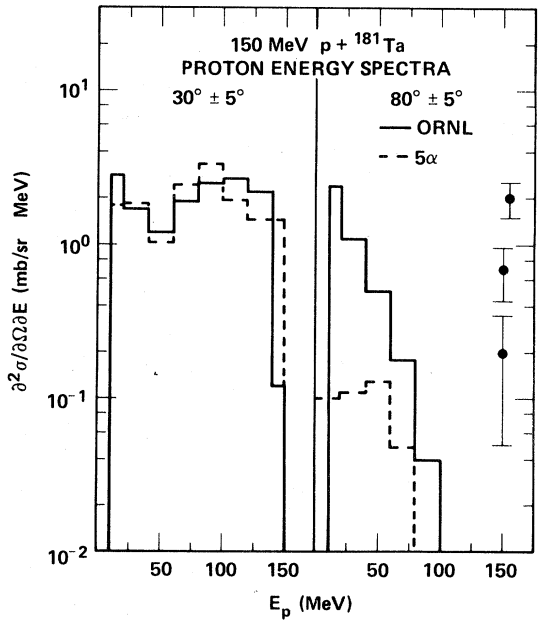

FIG. 4. Calculated energy spectra for protons emitted at 30° and 80° in the 150-MeV $p+^{181}$Ta system. See Fig. 2 for details.

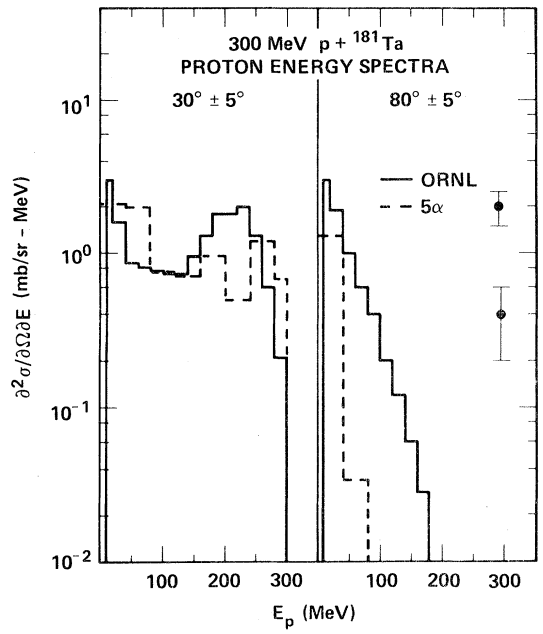

FIG. 5. Calculated energy spectra for protons emitted at 30° and 80° in the 300-MeV $p+^{181}$Ta system. See Fig. 2 for details.

cles with different masses and dynamic effects from the angular distributions; both of which are necessary to understand the changes apparent in Figs. 2–5.

For the 150-MeV $p+^{127}$Al (Fig. 2) case at 30° with clusters present there is a substantial contribution from single-scattering $p+\alpha$ collisions which produces a peak near 140-MeV proton energy. This occurs at the expense of multiple collisions so that fewer low-E protons are observed. On the other hand, at 80° there is little direct contribution to the energy distribution owing to single $p+\alpha$ scattering so that the spectrum is dominated by contributions from nucleon-nucleon multiple scattering.

Protons from 300-MeV $p+^{127}$Al (Fig. 3), on the other hand, exhibit a seemingly opposite effect at 30° than the 150-MeV results when clusters are needed. That is, fewer energetic protons are observed at 30°. This change we interpret as owing to the more forward-peaked angular distribution of the $p+\alpha$ collisions at 300 MeV so that there is at 300 MeV very little contribution from direct $p+\alpha$ scattering at 30°. Therefore, multiple scattering and $p+$nucleon collisions determine the spectrum.

Similar remarks and conclusions can be drawn from the $p+$Ta spectrum shown in Figs. 4 and 5 which are this time compared with results of the ORNL code.[8] The effects of clusters in Ta are less than Al in these calculations because even with five α's present in Ta the ratio of clusters to free nucleons is dramatically less for Ta. We include these figures to demonstrate the similarity with the ^{27}Al results and so that the reader may compare directly with the results from other cascade codes summarized in Ref. 8.

In general, the inclusion of deuteron clusters serves only to remove nucleons from the cascade without changing the resultant distributions. This is because of the relatively low breakup threshold of the deuteron. A more meaningful study of the role of preformed deuteron clusters will probably require that the nucleon cascade subsequent to the breakup also be followed. Since this option is not available in the present version of the code, a detailed study of the possible role of deuteron clusters is left to a later time. Nevertheless, owing to the relatively low binding energy of the deuteron we speculate that the presence of deuterons will not change the simple nucleon-nucleon cascade results much.

C. Residual spallation products

In Ref. 8 it was pointed out that some of the largest apparent differences between the various cascade codes were evident in the excitation energy distributions of the residual nuclei after the cascade. The same seems to be true when clusters are added. In Figs. 6 and 7 representative spectra are shown. In Fig. 6 the spectra of the (p,p'), (p,n), and (p,pn) residuals for cascades with no clusters all exhibit the same trend. This trend is a continual decrease

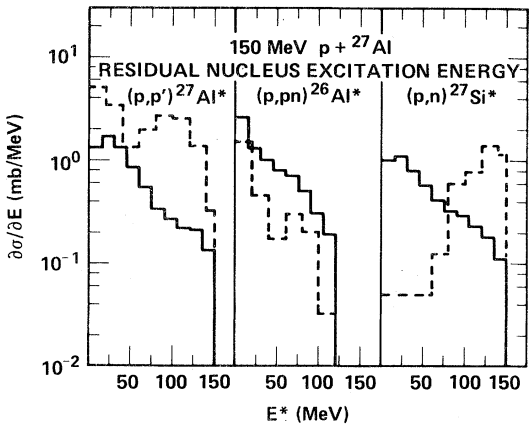

FIG. 6. Calculated residual nucleus excitation energy spectra for the 150-MeV $p+^{27}$Al reaction. The solid line is for no clusters in the target nucleus. The dashed line is from a cascade calculation which includes three alpha particles in the target nucleus.

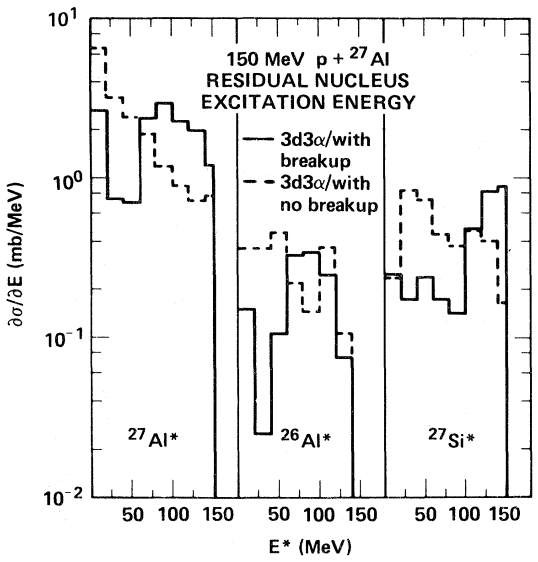

FIG. 7. Calculated residual nucleus excitation spectra with different assumptions about cluster breakup, as in Fig. 6.

in the number of residuals with higher excitation energies which can be related to the increased likelihood that an energetic cascade nucleon will escape rather than undergo enough cascade collisions to deposit all of its energy in the residual. When clusters are present, however, there is another possibility. A nucleon-cluster collision may induce a breakup. In the present version of the code this leads to a deposition of all of the nucleon energy into the residual. This is the origin of the energetic peak visible in the (p,p') and (p,n) spectra. The peak corresponds to an energetic particle colliding with a cluster after an initial collision which emits a proton or neutron. The fact that after two nucleons have been ejected there is less energy available for α-particle breakup is reflected in the diminished amplitude of the breakup contribution to the (p,pn) reaction. This conclusion is also supported by the spectra of Fig. 7 which show the differences in the residual excitation spectra when breakup of the clusters is not considered. Here both three deuterons and three alphas are permitted in the ^{27}Al target. When breakup is not allowed the spectra much more closely resemble the no-cluster spectra of Fig. 6.

As pointed out in the next section and discussed in Ref. 8, the distinction between the residual excitations may be somewhat academic in this cascade plus evaporation model since increased residual excitation energy will be compensated by increased particle evaporation at a higher temperature. The resultant mass-yield curves are therefore rather insensitive to whether or not clusters have been included in the target.

IV. REACTIONS INDUCED BY COMPLEX NUCLEI

In order to demonstrate the application of the CLUST model to reactions involving light ions other than protons, calculations for the systems 140-MeV ^{4}He incident on ^{27}Al and ^{233}U have been performed. In these comparisons the data of Hornyak *et al.*,[38] Wu *et al.*,[39] and Meyer *et al.*[40] have been used. In the calculations that follow, three special cases are considered: NC refers to no clusters preexisting in the target; NCNB is the same except that breakup of the incident α particle is ignored; 3α as in the previous sections denotes three alpha-particle clusters present in the target nucleus with breakup of these clusters and the incident projectile allowed.

A. Reaction cross sections and particle multiplicities

In Table III the alpha-particle reaction cross section and the cascade multiplicities of various particles are compared with the experimental data[37] for the 140-MeV $\alpha + ^{27}$Al reaction. Contrary to what was found in the proton-induced reactions, the ten-

TABLE III. Calculated and experimental (Ref. 38) reaction cross sections σ_R and average particle multiplicities (σ_i/σ_R) for the emission of cascade protons, $\bar{\nu}_p$; neutrons, $\bar{\nu}_n$; deuterons, $\bar{\nu}_d$; and alpha particles, $\bar{\nu}_\alpha$, of the 140 MeV + ^{27}Al reaction.

Projective	Target	Clusters	σ_R (mb)	ν_p	ν_n	ν_d	ν_α
140-MeV α	^{27}Al	NCNB	783	0.30	0.44	0	0.45
		NC	716	0.21	0.18	0	0.19
		3α	824	0.031	0.048	0	0.19
		exp	1141	0.29		0.18	0.24

dency here is to underestimate the reaction cross section. This suggests that perhaps more complex interactions than simple α-nucleon and α-α collisions contribute to the absorption of incident alpha particles. However, recent studies of the $\alpha+{}^{12}C$ system have reported smaller experimental cross sections than the calculations.[41] Hence, further experimental clarification of this point is needed. The cascade particle multiplicities, on the other hand, agree reasonably well with the data, although for NCNB ν_α is somewhat overestimated, as might be expected when breakup is ignored. Also, for the 3α, ν_p is underestimated again owing to the oversimplified assumption that breakup particles are removed from the cascade. Overall the NC and NCNB cases seem to reproduce the data equally well.

B. Charged particle spectra

Angle-integrated proton energy spectra for the model calculations and experiment are shown in Fig. 8 for 140-MeV $\alpha+{}^{27}Al$. The NC and NCNB cases fit the high-energy (>60 MeV) nonequilibrium region of the spectrum quite well. The 3α case does not reproduce this component because too many protons are absorbed by cluster breakup. The evaporation component (shown in Fig. 8 for NCNB only) also fits the low-energy equilibrium spectrum quite well for all three cases.

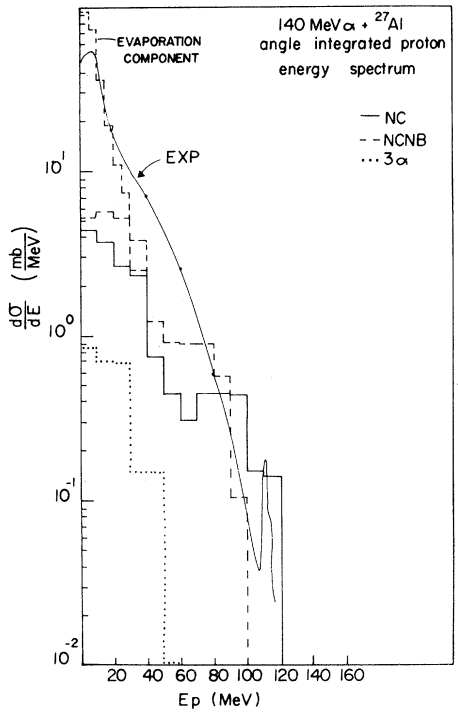

FIG. 8. Calculated and experimental angle-integrated proton energy spectrum for the 140-MeV $\alpha+{}^{27}Al$ reaction. Two low energy components are shown for the NCNB case; the lower curve is for NCNB alone, the upper curve includes the results of an evaporation calculation. Data are from Ref. 37.

The deficiency in the number of emitted protons in the 30–60 MeV region is expected since this is just the region where protons resulting from breakup of the incident alpha particles should appear. In the measurement of the 140-MeV $\alpha+{}^{27}Al$ system by Wu *et al.*,[39] a broad bump at an energy of about 35 MeV was observed in the proton energy spectra at forward angles and was also somewhat visible in the angle-integrated spectrum (Fig. 8). Since 35 MeV is one-fourth of the beam energy, it was concluded that these protons result from a breakup of the incident alpha particle into two or more particles with each having a share of the total kinetic energy proportional to its mass fraction of the projectile. This mechanism has recently been demonstrated to be valid in triple-coincidence studies between fission fragments and associated light ions.[42] If this interpretation is correct, then one can estimate[39] from the area under this bump that roughly 10% of the reaction cross section leads to this component of protons. This is substantially less than the fraction of incident alpha particles which break up in the calculation ($\sim 60\%$). The difference is presumably due to the fact that a significant fraction of the breakup nucleons undergo subsequent cascade interactions and are removed from the peak. This possibility can be better investigated when breakup nucleons are permitted in the cascade. To some extent this difference may also be due to the uncertainty[39] of estimating the area of the breakup peak which rapidly increases and shifts to lower energy at forward angles.

Figure 9 shows the angle-integrated alpha-particle energy spectrum for the 140 MeV ${}^4He+{}^{27}Al$ system. The experimental distribution from Ref. 38 is essentially composed of a low-energy evaporation component plus a relatively flat nonequilibrium (or cascade) component which extends up to the discrete-state contribution at the highest energies. A difference in the calculated cascade as breakup (NC) and clusters (3α) are added can be seen as a decrease in the emission of alpha particles with energies of $\sim 40-60$ MeV. This part of the spectrum, which is presumably due to incident alpha particles which have experienced several $\alpha+$nucleon collisions, is not recovered when

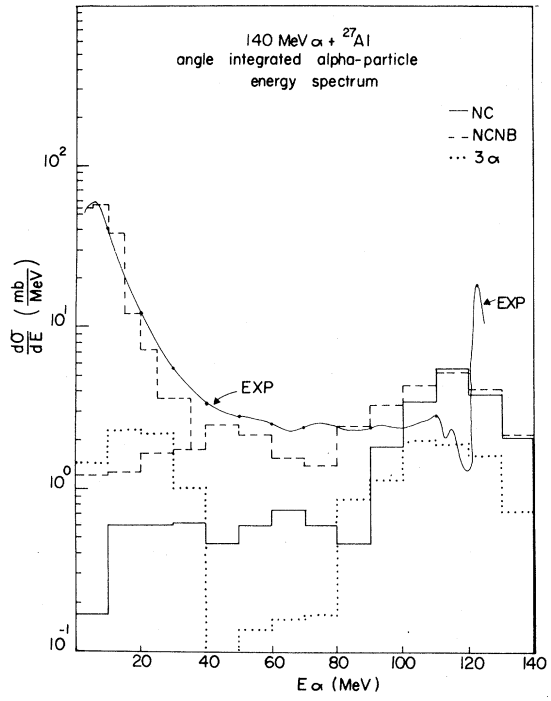

FIG. 9. Calculated experimental angle-integrated alpha-particle energy spectrum for the 140-MeV $\alpha+^{27}$Al reaction. Data are from Ref. 39.

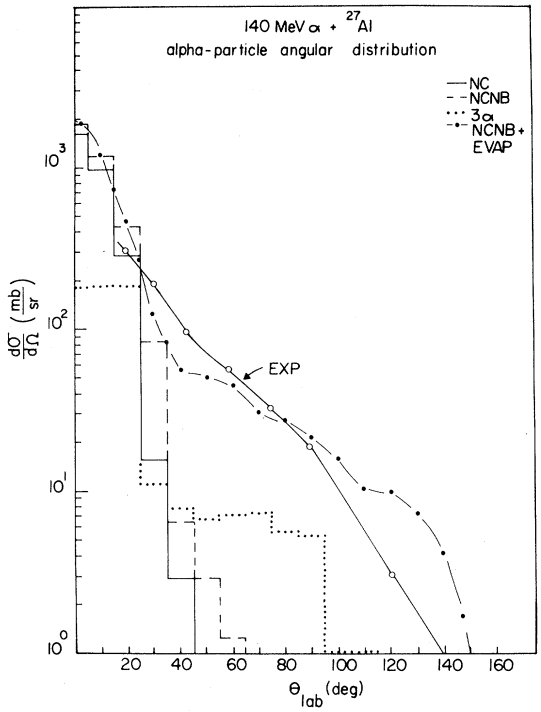

FIG. 10. Calculated and experimental alpha-particle angular distribution for the 140-MeV $\alpha+^{27}$Al reaction. Data from Ref. 39.

the evaporation component is added. The evaporation component (shown for the NCNB case only) introduces low energy (<40 MeV) particles. It is found that the evaporation code fits the low energy part of the spectrum well, no matter which assumptions are made about clustering and/or breakup in the CLUST calculation. This is owing to the fact that as the low energy component of the particle spectrum becomes more depleted (as in the cases for increasing amounts of clustering), the residual nuclei have higher excitation energies. Therefore, in the evaporation stage more particles are emitted, which tends to compensate for the underproduction in the cascade step. The overall fit for the NCNB case is remarkably good, suggesting that alpha-particle breakup may be overestimated in the simple model applied here.

Figure 10 shows the angular distributions of alpha particles as calculated by the CLUST code along with the experimentally measured distribution. The distribution is very forward-peaked for all cases. The addition of clusters (3α) shows a tendency to spread out and diminish the cascade distribution, although when the evaporation component is added there is not much distinction between the angular distributions from all three cases. The result of adding the evaporation component in the NCNB calculation is also shown on Fig. 10. The fit to the experimental data is quite good, except perhaps for the most backward angles where the evaporation code slightly overestimates the yield.

C. Residual products

The predictions for the excitation energy spectra of the major residual spallation products from the 140 MeV $\alpha+^{27}$Al reaction are shown in Figs. 11 and 12. It can be seen in these figures that for simple knockout reactions [e.g., (α,n) and (α,p)] the excitation energy spectra are peaked near the maximum permissable value. This spectral shape indicates that the incident alpha particles transfer only a small amount of their kinetic energy to the struck nucleons. The alpha particle is then adsorbed by the target nucleus with its kinetic energy going into thermal excitation of the residual. For reactions involving the emission of an alpha particle [e.g., (α,α') and $(\alpha,\alpha'n)$ shown in Fig. 12] one can see that the excitation energy of the residuals is peaked at very low energies. This behavior indicates a single low-energy transfer collision with a nucleon, re-

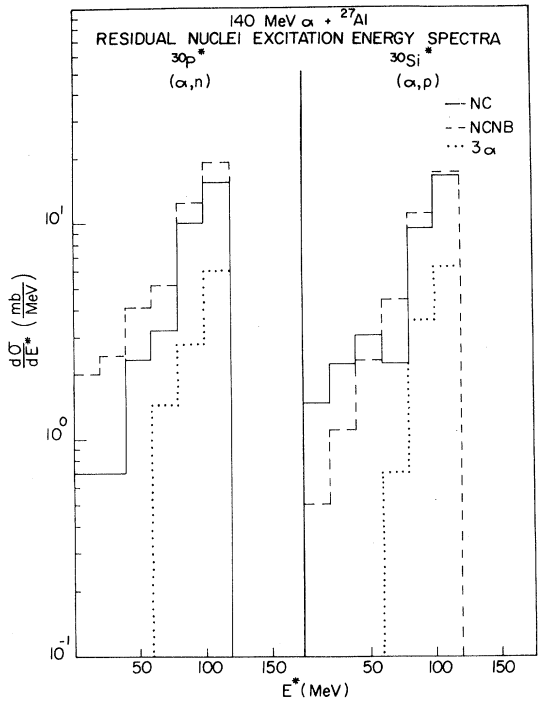

FIG. 11. Calculated residual nucleus excitation energy spectra for the 140-MeV $\alpha+^{27}$Al reaction.

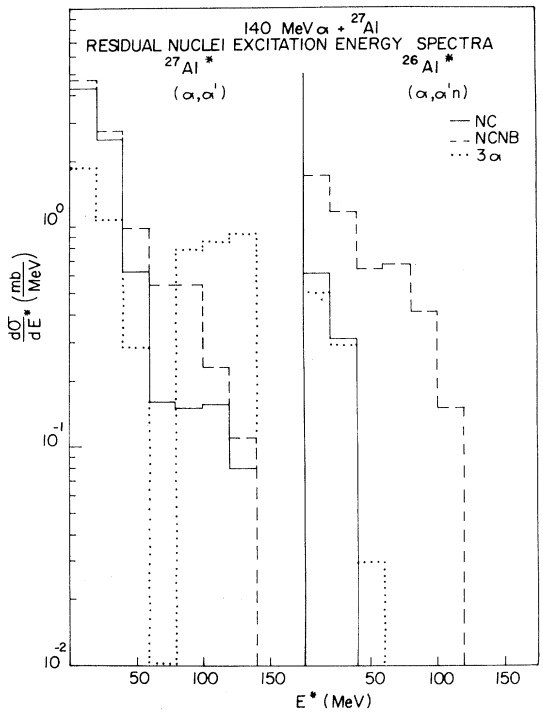

FIG. 12. Calculated residual nucleus excitation energy spectra for the 140-MeV $\alpha+^{27}$Al reaction.

sulting in the survival and subsequent emission of the incident alpha particle. By adding three alpha-particle clusters to the target nucleus, the ^{27}Al* spectrum shows an enhancement for high excitation energies, again demonstrating the energy damping associated with collisions involving target clusters.

Figure 13 shows the mass distribution for a combined cascade-evaporation calculation for the 140-MeV $\alpha+^{27}$Al system, which is compared with measurements of Hornyak *et al.* (38). As in the $p+^{27}$Al reaction, for $\alpha+^{27}$Al there is little effect on the final distribution of nuclei when clusters are added. Hence, for simplicity, only the breakup and no breakup case are shown. The breakup and no breakup cases show little difference in the residual mass yield except for a slight enhancement in mass near the $A\cong 14-16$ region for the breakup-allowed case. The increased yield in this region is owing to the larger number of compound nuclei with high excitation energy ($\sim$140 MeV) that are formed when breakup is allowed. These data compare much more favorably with the experimental results than do predictions of the preequilibrium decay codes,[38] in which too much yield is predicted in the $A=20-24$ region with a cutoff at about $A=15$.

Another indication that alpha-particle breakup is overestimated in the code is indicated in Fig. 14 which shows fission fragment angular correlations

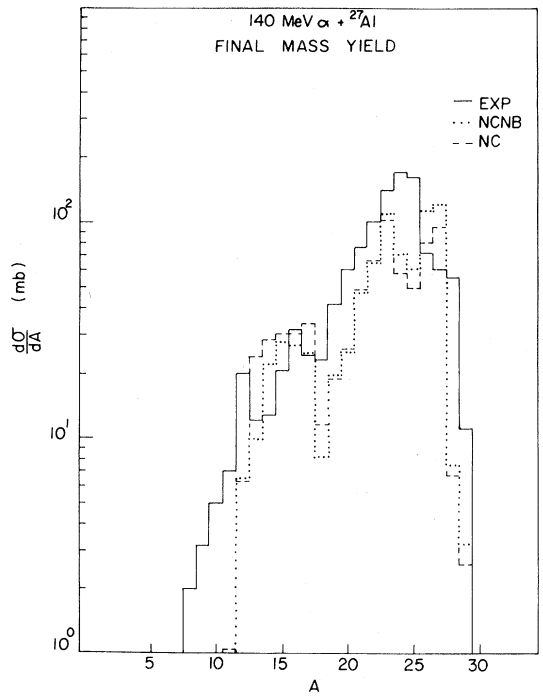

FIG. 13. Calculated and experimental mass yields for the 140-MeV $\alpha+^{27}$Al reaction. Data are from Ref. 38.

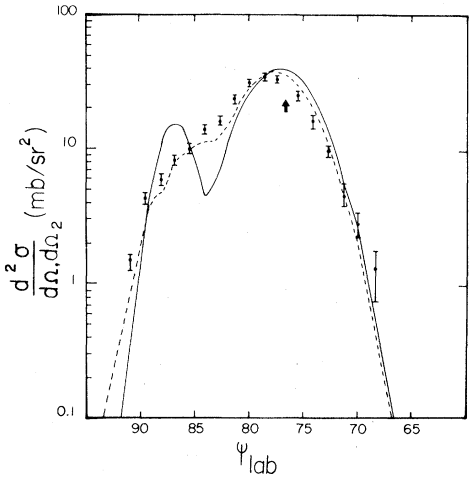

FIG. 14. Comparison of the experimental fission fragment angular correlations for 140-MeV $\alpha+^{233}$U with predictions based on the intranuclear cascade model. The solid line refers to cascades which allow alpha-particle breakup; the dashed line refers to a no-breakup assumption.

from the 140-MeV $\alpha+^{233}$U reaction.[39] These correlations measure the linear momentum transfer of the incident projectile to the target nucleus which later fissions. The more forward-angle peak corresponds to large linear momentum transfers. The arrow indicates the angle at which the alpha particle is completely absorbed, followed by symmetric fission. The NCNB (dashed) curve fits the data much better than the NC (solid curve). The difference is due to collisions in which breakup causes the alpha particle to be completely absorbed into a compound nucleus. This results in a clearer distinction between the direct and compound-nuclear components. Again, this discrepancy can probably be eliminated when the breakup is treated more realistically. The implication from the present version of the code, however, is that the best fits are obtained when alpha-particle breakup into four nucleons is ignored.

V. CONCLUSIONS

The previous sections have described a modified version of the intranuclear cascade code which introduces deuteron and alpha-particle clusters into the intranuclear cascade, both as incident projectiles and as components of the target nucleus. For proton-induced reactions the introduction of clusters in the target nucleus tends to increase the reaction cross sections and can enhance the emission of high energy protons, but decrease the average number of particles emitted during the cascade. One deficiency of intranuclear cascade codes has always been the underproduction of high energy particles. Hence, the inclusion of clusters would seem to be a first step in the correct direction. Also, it was found that even though increased clustering could produce a decrease in the number of low energy protons, the excitation energy of the residual nuclei is enhanced which leads to emission of more low energy particles in the evaporation phase of the reaction. In terms of the overall reproduction of experimental data, it appears at this time, however, that there is little direct evidence of the need to introduce clusters in the target nucleus, although this is a question which merits further study and more detailed comparisons with experimental data.

Although the inclusion of clusters in the cascade model represents a more realistic physical picture for the description of intermediate-energy nuclear reactions, it requires additional parametrization in that spectroscopic factors for the existence of clusters in the target nucleus are needed. This information can hopefully be provided by quasifree scattering experiments or appropriate nuclear shell-model calculations. However, the use of such data requires a better knowledge of the cluster density distribution.

Perhaps the most significant advantage of the CLUST code is that calculations can now be made with the intranuclear cascade model for reactions induced by deuteron and alpha-particle projectiles. A reasonable understanding of the data from alpha-induced collisions can be made in terms of an intranuclear cascade including complex particles plus evaporation. The gross features of the data are well reproduced. It seems that the present version of the model is basically insensitive to whether or not the incident projectile is allowed to break up during the collision, although the no-breakup situation is perhaps slightly favored as far as the overall reproduction of the data is concerned (particularly for the alpha particle energy spectrum). On the other hand, there is a need, particularly evident in the proton energy spectra, to consider projectile breakup and the subsequent fate of the cascade particles after the breakup.

The overall fit to the 140-MeV $\alpha+^{27}$Al experimental data is an encouraging aspect of the present calculations because the cascade-evaporation code has the advantage of including kinematic factors for the products. Thus, it permits a straightforward calculation of angular distributions and energy

spectra for residual product nuclei and may provide a better kinematical description than in preequilibrium exciton model calculations. Comparisons with experimental data of this sort constitute a more sensitive test of the theoretical model, and hence may evaluate the nuclear parameters more critically than may be possible with the preequilibrium exciton model.

Further improvements to the model still need to be considered; for example, coalescence of outgoing nucleons in the cascade, inclusion of Coulomb deflection of the clusters and nucleons, and most importantly the evolution of the cascade after projectile breakup.

In conclusion, the CLUST code provides a substantially broader application of the intranuclear cascade model. It provides increased sensitivity of the model for light target nuclei and provides the important generalization of the model to deuteron- and alpha-particle-induced reactions. In a forthcoming paper further applications of the CLUST code will include a detailed comparison of the model with the extensive experimental data from the $p+{}^{12}C$, $p+{}^{16}O$, and $\alpha+{}^{12}C$ reactions at bombarding energies between 40—100 MeV for protons and 40—160 MeV for alpha-particle-induced reactions.

ACKNOWLEDGMENTS

This work was supported by the U. S. Department of Energy. The authors wish to acknowledge the contribution of the late N. S. Wall to this work. We also thank W. F. Hornyak, C. Butterfield, and A. Gökmen for assistance at different points in this work. The support of the University of Maryland Science Center, where these calculations were performed, is also gratefully acknowledged.

[1]R. Serber, Phys. Rev. 72, 1114 (1947).
[2]M. L. Goldberger, Phys. Rev. 73, 1269 (1948).
[3]N. Metropolis, R. Bivins, M. Storm, A. Turkevich, J. M. Miller, and G. Friedlander, Phys. Rev. 110, 85 (1958); 110, 204 (1958).
[4]H. W. Bertini, Phys. Rev. 131, 1801 (1963).
[5]E. Gradsztajn, Ann. Phys. (Paris) 10, 791 (1965).
[6]J. P. Cohen, Nucl. Phys. 84, 316 (1966).
[7]K. Chen, Z. Fraenkel, G. Friedlander, J. R. Grover, J. M. Miller, and Y. Shimamoto, Phys. Rev. 166, 949 (1968).
[8]V. S. Barashenkov, H. W. Bertini, K. Chen, G. Friedlander, G. D. Harp, A. S. Iljinov, J. M. Miller, and V. D. Toneev, Nucl. Phys. A187, 5331 (1972).
[9]I. Dostrovsky, Z. Fraenkel, and G. Friedlander, Phys. Rev. 116, 683 (1960).
[10]E. Gradsztajn, Phys. Rev. Lett. 13, 240 (1964).
[11]G. Ripka, *Advances in Nuclear Physics* (Plenum, New York, 1968), Vol. 1.
[12]D. M. Brink and J. J. Castro, Nucl. Phys. A216, 109 (1973).
[13]N. S. Chant and P. G. Roos, Phys. Rev. C 15, 57 (1977).
[14]J. G. Rogers, G. Paic, M. B. Epstein, J. W. Verba, and J. R. Richardson, *Three-Body Problem in Nuclear and Particle Physics,* Birmingham, 1969, edited by J. S. C. McKee and P. M. Rolph (North-Holland, Amsterdam, 1970), p. 414.
[15]I. Slaus, *Three-Body Problem in Nuclear and Particle Physics,* Birmingham, 1969, edited by J. S. C. McKee and P. M. Rolph (North-Holland, Amsterdam, 1970), p. 337.
[16]C. C. Kim, Nucl. Phys. 58, 32 (1964).
[17]A. S. Wilson, M. C. Taylor, J. C. Letg, and G. C. Phillips, Nucl. Phys. A126, 193 (1969).
[18]R. L. Schulte, M. Cosack, A. W. Obst, and J. L. Weil, Nucl. Phys. A192, 609 (1972).
[19]A. D. Bacher and T. A. Tombrello, Nucl. Phys. A113, 557 (1968).
[20]I. Reichstein and Y. C. Tang, Nucl. Phys. A158, 529 (1970).
[21]E. T. Boschitz, W. K. Roberts, J. S. Vincent, M. Blecher, K. Gotow, P. C. Gugelot, C. F. Perdrisat, L. W. Swenson, and J. R. Priest, Phys. Rev. C 6, 457 (1972).
[22]O. N. Jarvis and C. Whitehead, Nucl. Phys. A184, 615 (1972).
[23]B. W. Davies, M. K. Craddock, R. C. Hanna, Z. J. Moroz, and L. P. Robertson, Nucl. Phys. A97, 241 (1967).
[24]D. Garetta, J. Sura, and A. Tarrats, Nucl. Phys. A132, 204 (1969).
[25]R. A. Arndt, L. D. Roper, and R. L. Shotwell, Phys. Rev. C 3, 2100 (1971).
[26]A. D. Bacher, G. R. Plattner, H. E. Conzett, D. J. Clark, H. Grunder, and W. E. Tivol, Phys. Rev. C 5, 1147 (1972).
[27]G. S. Mani and A. Tarratts, Nucl. Phys. A107, 625 (1968).
[28]I. Brissaud, M. K. Brussel, M. Sowinski, and B. Tatischeff, Phys. Lett. 30B, 324 (1969).
[29]J. H. Jett, J. L. Detch, Jr., and N. Jarmie, Phys. Rev. C 3, 1769 (1971).
[30]M. T. Collins and J. J. Griffin, Nucl. Phys. 348, 63 (1980); J. J. Griffin, in *Clustering Aspects of Nuclear Structure and Nuclear Reactions (Winnipeg, 1978),* Proceedings of the Third International Conference on Clustering Aspects of Nuclear Structure and Nuclear reactions, edited by W. H. T. Van Oers, J. P. Svenne,

J. S. C. McKee, and W. R. Falk (AIP, New York, 1978), p. 114.
[31]E. Gradsztajn, F. Yiou, R. Klapisch, and R. Bernas, Phys. Rev. Lett. 14, 436 (1965).
[32]A. Gökmen, Ph.D. thesis, University of Maryland, 1981.
[33]V. S. Barashenkov, K. K. Gudima, and V. D. Toneev, Acta. Phys. Pol. 36, 415 (1969).
[34]A. Johansson, U. Svanberg, and O. Sundberg, Ark. Fys. 19, 527 (1961).
[35]V. Comparat, R. Frascaria, N. Marty, M. Morlet, and A. Willis, Nucl. Phys. A221, 403 (1974).
[36]G. P. Milburn, W. Birbaum, W. E. Crandall, and L. Schechter, Phys. Rev. 95, 1268 (1954).
[37]H. H. Gutbrod, A. Sandoval, P. J. Johansen, A. M. Poskanzer, J. Gosset, W. E. Meyer, G. D. Westfall, and R. Stock, Phys. Rev. Lett. 37, 667 (1976).
[38]W. F. Hornyak, M. D. Glascock, C. C. Chang, and J. R. Wu, Phys. Rev. C 19, 1595 (1979).
[39]J. R. Wu, C. C. Chang, and H. D. Holmgren, Phys. Rev. C 19, 1595 (1979).
[40]W. G. Meyer, V. E. Viola, Jr., R. G. Clark, and S. M. Read, Phys. Rev. C 20, 1716 (1979).
[41]A. Gökmen, H. Breuer, B. Glagola, A. C. Mignerey, K. Kwiatkowski, and V. E. Viola (unpublished).
[42]K. K. Kwiatkowski, V. E. Viola, Jr., H. Breuer, C. C. Chang, A. C. Cowley, H. D. Holmgren, and A. C. Mignerey (unpublished).